



## Differential activation of the mTOR/autophagy pathway predicts cognitive performance in APP/PS1 mice



Rasika S. Vartak<sup>a</sup>, Alexis Rodin<sup>a</sup>, Salvatore Oddo<sup>a,b,\*</sup>

<sup>a</sup> Arizona State University-Banner Neurodegenerative Disease Research Center, Biodesign Institute, Arizona State University, Tempe, AZ, USA

<sup>b</sup> School of Life Sciences, Arizona State University, Tempe, AZ, USA

### ARTICLE INFO

#### Article history:

Received 22 February 2019  
Received in revised form 19 July 2019  
Accepted 17 August 2019  
Available online 3 September 2019

#### Keywords:

Alzheimer's disease  
AD  
Plaques  
Tangles  
tau  
A $\beta$

### ABSTRACT

The molecular bases underlying cognitive impairments in Alzheimer's disease remain elusive. In this study, we sought to determine the molecular correlates of memory deficits in APP/PS1 mice, a widely used animal model of Alzheimer's disease. To this end, we tested 18-month-old APP/PS1 mice in the Morris water maze and ranked them by their spatial memory performance. We found that some APP/PS1 mice performed poorly, whereas others performed as well as nontransgenic mice. We took advantage of this intragroup variability to identify the best predictor of cognitive deficits. In this APP/PS1 cohort, soluble and insoluble amyloid- $\beta$  levels did not correlate significantly with cognitive performance. However, we found that cognitive performance within the APP/PS1 group had a strong inverse correlation with A $\beta$  plaque load and mammalian target of rapamycin activation and positively correlated with autophagy activation. Our data suggest that mammalian target of rapamycin signaling may account cognitive performance in APP/PS1 mice.

© 2019 Elsevier Inc. All rights reserved.

### 1. Introduction

Alzheimer's disease (AD) is the most common neurodegenerative disorder in the United States, with an estimated 5.4 million currently diagnosed cases (Alzheimer's Association, 2016). Although most of the cases are sporadic and of an unknown etiology, less than 5% of cases are caused by mutations in either the amyloid precursor protein (APP) gene or the genes encoding presenilin 1 or 2 (Masters et al., 2015). Neuropathologically, AD is characterized by the accumulation of extracellular amyloid plaques and neurofibrillary tangles, as well as neuronal loss, brain atrophy, and chronic inflammation. Plaques are mainly made of amyloid- $\beta$  (A $\beta$ ), a short peptide that is derived from the proteolytic processing of the APP; tangles are made of hyperphosphorylated tau. Overwhelming evidence suggests that A $\beta$  and tau play a significant role in the pathogenesis of the disease by mechanisms that are not clearly understood.

Aging is the major risk factor for AD and the percentage of people with AD increases dramatically with age. To this end, 81% of the currently estimated number of people living with AD in the United States is 75 years or older (Hebert et al., 2013; Masters et al., 2015). However, little is known about the mechanisms by which aging

affects the onset of AD pathology. Converging evidence indicates that the mammalian target of rapamycin (mTOR) plays a crucial role in aging (Razquin Navas and Thedieck, 2017; Richardson et al., 2015). To this end, reducing mTOR activity in animal models, including rodents, Drosophila, and yeast, increases lifespan (Bjedov et al., 2010; Harrison et al., 2009; Jia et al., 2004; Radde et al., 2006). mTOR is a ubiquitously expressed kinase that regulates protein translation and cell proliferation (Wullschlegler et al., 2006). Hyperactive mTOR signaling has been shown in brain regions affected by AD (An et al., 2003; Caccamo et al., 2015; Li et al., 2005). Consistent with these observations, decreasing mTOR signaling in animal models of AD reduces AD-like pathology and improves cognition (Caccamo et al., 2013, 2014; Jia et al., 2004; Lafay-Chebassier et al., 2005; Oddo, 2012; Talboom et al., 2015). One way by which mTOR may regulate aging and contribute to AD is by its role in insulin signaling (Caccamo et al., 2018; Norambuena et al., 2017; Orr et al., 2014; Velazquez et al., 2017). To this end, direct manipulation of insulin signaling regulates lifespan (Gkikas et al., 2014; Kenyon et al., 1993). Notably, insulin dysregulation has been reported in AD and animal models of AD (Folch et al., 2018; Rodriguez-Rivera et al., 2011; Velazquez et al., 2017). Although the role of mTOR and insulin signaling pathways in AD pathology is just coming to light, it is unknown whether dysregulation of these pathways is associated with cognitive impairment. In this study, we identify the molecular pathways that best correlate with cognitive function in 18-month-old APP/PS1 mice, a widely used animal model of AD.

\* Corresponding author at: Neurodegenerative Disease Research Center, Biodesign Institute, School of Life Sciences, Arizona State University, 1001 S McAllister Ave, Tempe, AZ, 85287. Tel.: +480-727-3490.

E-mail address: [oddo@asu.edu](mailto:oddo@asu.edu) (S. Oddo).

## 2. Materials and methods

### 2.1. Mice

We purchased the APP/PS1 from The Jackson Laboratory (stock number 017009) and backcrossed them to 129/SvJ mice for more than 12 generations. All mice used in this study were littermates. Mice were housed 4–5 per cage, kept on a 12-hour light/dark cycle, and given *ad libitum* access to food and water. Animal care and treatments were according to the regulations of The Institutional Animal Care and Use Committee of Arizona State University.

### 2.2. Morris water maze

The Morris water maze (MWM) test was performed as described before (Branca et al., 2014) and was used to assess spatial cognition and memory in 18-month-old APP/PS1 mice and nontransgenic (NonTg) mice. Briefly, mice were trained in a circular tank for 4 trials per day for 5 days to find a hidden platform beneath the water. Escape latency and distance traveled to find the platform were measured for each mouse. On day 6, the platform was removed, and mice were allowed to swim freely for 60 seconds. During this time, the number of platform location crosses and the time to reach the platform were measured. MWM data were analyzed using EthoVision XT tracking system (Noldus Information Technology, VA, USA).

### 2.3. Protein extraction

Mice were sacrificed by cervical dislocation and their brains were removed and bisected sagittally. One half was fixed in phosphate-buffered saline with 4% paraformaldehyde for 48 hours after which it was transferred to phosphate-buffered saline with 0.2% sodium azide. The other half was frozen and homogenized in Tissue Protein Extraction Reagent (Thermo Fisher Scientific) containing protease (Roche Applied Science, USA) and phosphatase (Millipore, USA) inhibitors. The soluble supernatant was centrifuged at 4 °C at 100,000 g for 1 hour and then stored at –80 °C. The pellet was homogenized in 70% formic acid, centrifuged as mentioned previously, and the supernatant was stored at –80 °C as the insoluble fraction.

### 2.4. Immunohistochemistry

A $\beta$  plaques were stained using a method described previously (Caccamo et al., 2018). Briefly, sections were washed in tris-buffered saline (TBS; 100 mM Tris pH 7.4, 150 mM NaCl) and incubated for 30 minutes in 3% H<sub>2</sub>O<sub>2</sub>, to quench endogenous peroxidase activity. Sections were then transferred into TBS-A (100 mM Tris pH 7.4, 150 mM NaCl, 0.1% Triton X-100) and TBS-B (100 mM Tris pH 7.4, 150 mM NaCl, 0.1% Triton X-100, 2% bovine serum albumin) for 15 and 30 minutes, respectively. Sections were then incubated overnight with an A $\beta$ 42-specific antibody. Sections were washed to remove excess antibody and incubated in the suitable secondary antibody for 1 hour at room temperature. Signal was enhanced by incubating sections in the avidin-biotin complex (Vector Labs, Burlingame, CA, USA) for 1 hour. Sections were then washed and developed with diaminobenzidine substrate using the avidin-biotin horseradish peroxidase system (Vector Labs). Images were obtained from 3 sections per animal with a digital Zeiss camera. Sections with full hippocampus were selected from anterior to posterior. Area of interest was drawn around the cortex or hippocampus for each section, and the percent area covered by plaques throughout the cortex or hippocampus was quantified using the “Analyze particle” function in Fiji.

### 2.5. Western blots

Proteins from soluble fractions were resolved by 10% Bis Tris SDS-polyacrylamide gel electrophoresis (ThermoFisher Scientific) under reducing conditions and transferred to a nitrocellulose membrane as per the manufacturer’s protocol. Membranes were then incubated with appropriate primary and secondary antibodies as described before (Belfiore et al., 2019). All primary antibodies were used at 1:1000 concentration, unless specified, whereas secondary antibodies were used at 1:10,000 concentration.

### 2.6. ELISA

We measured A $\beta$ 40 and A $\beta$ 42 levels in the soluble and the insoluble fractions by enzyme-linked immunoassay (ThermoFisher Scientific) using the manufacturer’s instructions.

### 2.7. Antibodies

From cell signaling, we used anti-Actin (#3700), mTOR (#2983), p-mTOR (#2971, 1:500), S6K1 (#9202), p-S6K1 (#9205), rpS6 (#2217), p-rpS6 (#5364), Atg5 (#2010), Atg7 (#2631), Beclin-1 (#3738), AMPK alpha (#2603), p-AMPK alpha (#2535), Akt (#2965), p-Akt (#9271), p-Akt (#2965), IRS-1 (#3407), p-IRS1 (#3203), PDK1 (#3062), and p-PDK1 (#3438). From Millipore, we used A $\beta$ 42 (#AB5078P). From BioLegend, we used 6E10 (#803003). From Sigma, we used APP C-terminal antibody (#A8717).

### 2.8. Statistics

All data were analyzed using GraphPad Prism (GraphPad Software, CA, USA, [www.graphpad.com](http://www.graphpad.com)). For behavior analysis, data were analyzed by two-way analysis of variance followed by Bonferroni’s correction, when required. Linear correlation analysis was run to obtain the Pearson’s correlation coefficient between platform crosses and protein levels or plaque load, as indicated. Student’s t-test was performed for percent area of A $\beta$  plaques in the hippocampus and cortex. Correction for multiple testing of hypothesis on the correlation with platform crosses in APP/PS1 mice was performed using Benjamini, Krieger, and Yekutieli method using  $Q = 5\%$ .

## 3. Results

### 3.1. Variation in cognitive performance within the APP/PS1 cohort

APP/PS1 mice overexpress the APP and the PSEN1 transgenes carrying familial AD mutations (Jankowsky et al., 2004). Cognitive deficits in APP/PS1 mice are first apparent at 7 months of age and progress as a function of age (Radde et al., 2006; Serneels et al., 2009). To identify the molecular pathways that may account for cognitive dysfunction in AD, we first assessed spatial learning and memory in 18-month-old APP/PS1 mice using the MWM. We trained APP/PS1 ( $n = 17$ ) and NonTg ( $n = 19$ ) mice for 5 consecutive days with 4 trials per day to find a hidden platform in the water. When we analyzed the time taken to find the hidden platform, we found a significant effect for days [ $p < 0.0001$ ;  $F(4, 136) = 34.60$ ] and genotype [ $p < 0.0001$ ;  $F(1, 136) = 35.94$ ], as well as a significant days/genotype interaction [ $p < 0.05$ ;  $F(4, 136) = 2.95$ ; Fig. 1A]. The day effect indicates that all mice learned the task, whereas the genotype effect indicates that the 2 genotypes learned at a different pace. Post hoc analysis indicated that APP/PS1 mice performed worse than the NonTg mice at days 3, 4, and 5 ( $p < 0.0001$ ; Fig. 1A). We obtained similar results for distance traveled to find the hidden platform with a significant effect found for days [ $p < 0.0001$ ;  $F(4, 136) = 40.75$ ] and genotype [ $p < 0.01$ ,  $F(1, 136) = 11.22$ ], as well as

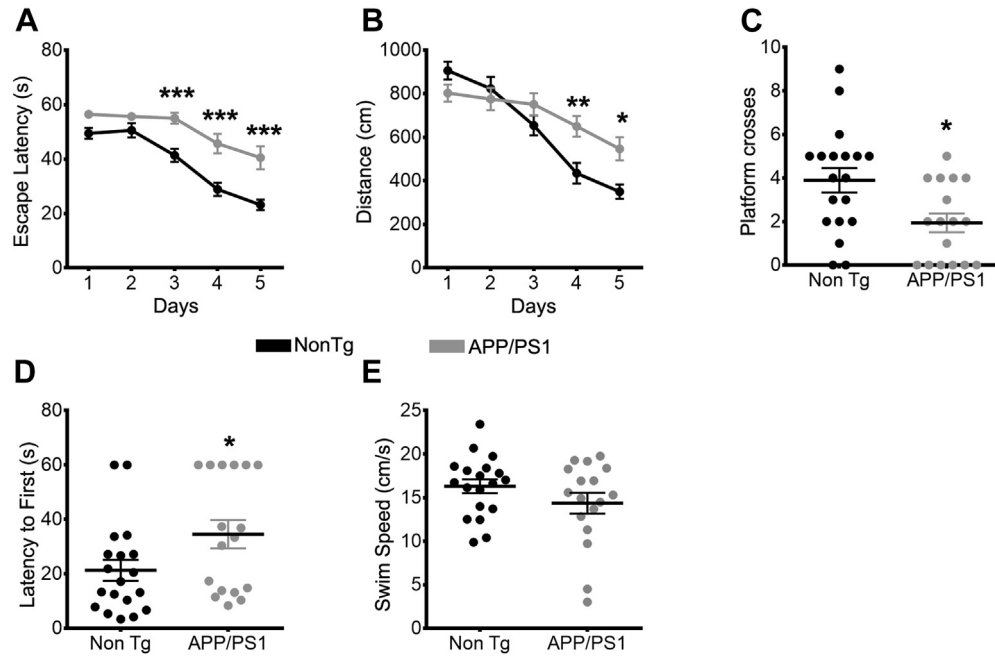


**Fig. 1.** Cognitive defects in APP/PS1 mice. (A and B) Learning curves of 18-month-old mice during the MWM test (APP/PS1,  $n = 17$ , NonTg,  $n = 19$ ). Each day represents the average of 4 training trials. For the escape latency, we found a significant effect for day, genotype, and days  $\times$  genotype interaction [day effect:  $p < 0.0001$ ;  $F(4, 136) = 34.60$ ; genotype effect:  $p < 0.0001$ ;  $F(1, 136) = 35.94$ ; interaction  $p < 0.05$ ;  $F(4, 136) = 2.95$ ]. APP/PS1 mice were impaired at day 3, 4, and 5. For the distance traveled to find the platform, we found a significant effect for day, genotype, and days  $\times$  genotype interaction [day effect:  $p < 0.0001$ ;  $F(4, 136) = 40.75$ ; genotype effect  $p < 0.01$ ,  $F(1, 136) = 11.22$ ; interaction  $p < 0.01$ ,  $F(4, 136) = 4.66$ ]. Data were analyzed by two-way analysis of variance. (C and D) The graph shows a significant difference between APP/PS1 and nontransgenic mice in the numbers of platform location crosses and time to find the first cross of the platform location, respectively, during a single 60-second probe trial ( $p < 0.05$ ). (E) Average swim speed during the probe trials was not significantly different between the 2 groups. The data in panels C–E were analyzed by unpaired Student's *t*-test. Abbreviations: MWM, Morris water maze; NonTg, nontransgenic. \* $p < 0.05$ ; \*\* $p < 0.01$ ; \*\*\* $p < 0.001$ .

significant days/genotype interaction [ $p < 0.01$ ,  $F(4, 136) = 4.66$ ; Fig. 1B]. Post hoc analysis showed a significant difference between the 2 groups at day 4 ( $p < 0.01$ ) and day 5 ( $p < 0.05$ ; Fig. 1B). Twenty-four hours after the last trial, the hidden platform was removed and we conducted a probe trial to assess spatial memory. We found that the total number of platform crosses ( $p < 0.05$ ;  $t = 2.75$ ) and escape latency to the platform ( $p < 0.05$ ;  $t = 2.081$ ) was significantly different between the 2 genotypes (Fig. 1C–D). In contrast, the swim speed between the 2 groups did not differ significantly (Fig. 1E). Further analysis of the probe trials indicated a large variability in the performance of APP/PS1 mice, with some mice that performed as well as NonTg mice (high-performance group), whereas others did not cross the platform location a single time (low-performance group).

### 3.2. $A\beta$ plaque load inversely correlates with cognitive performance in APP/PS1

We sought to determine the molecular basis underlying the difference in spatial memory between the low- and the high-performance groups. We defined the high-performance group as APP/PS1 mice that crossed the platform location  $\geq 4$  times during the probe trial ( $n = 5$ ). By contrast, the APP/PS1 mice that did not cross the platform location during the probe trials represent the low-performance group ( $n = 6$ ). We first assessed whether sex was related to performance but found no significant correlation between the 2 groups ( $r = 0.03$ ,  $p = 0.98$ ).  $A\beta$  plaque deposits are a hallmark of AD pathology and have been linked to cognitive decline (Foley et al., 2015; Huber et al., 2018; Nelson et al., 2009). We sought to determine whether  $A\beta$  pathology could account for the difference in spatial memory between the low and high performing 18-month-old APP/PS1 mice. We found that  $A\beta$  plaque load was

significantly lower in the cortex and hippocampus of the high-performance mice compared with the low-performance mice (Fig. 2A–B). We then performed a correlation analysis between  $A\beta$  plaque load and platform location crosses in all 18-month-old APP/PS1 mice. We found a significant negative correlation between  $A\beta$  plaque load and platform frequency in both the cortex ( $r = -0.765$ ,  $p < 0.001$ ,  $q < 0.01$ ) and hippocampus ( $r = -0.621$ ,  $p < 0.05$ ,  $q < 0.05$ ; Fig. 2C–D, Table 1). To further evaluate the link between  $A\beta$  and cognition in APP/PS1 mice, we measured soluble and insoluble  $A\beta_{40}$  and  $A\beta_{42}$  levels by sandwich enzyme-linked immunoassay, again using all the APP/PS1 tested behaviorally. We did not find any significant correlation between platform location crosses and the levels of soluble and insoluble  $A\beta_{40}$  and  $A\beta_{42}$  (Fig. 2E–H). To evaluate whether there was a link between APP processing and spatial memory, we measured the levels of full-length APP and its C-terminal fragments by Western blot. We found no significant correlation between platform crosses and APP, C99, and C83 levels (Fig. 3A–D). These data indicate that, in old APP/PS1 mice, cognitive function inversely correlates with  $A\beta$  plaque load but not with APP levels or processing.

### 3.3. Insulin signaling does not correlate with cognitive performance in APP/PS1 mice

A growing body of evidence suggests that insulin signaling may be linked to AD pathogenesis (Folch et al., 2018; Rodriguez-Rivera et al., 2011; Velazquez et al., 2017). We thus assessed whether changes in insulin signaling could account for the differential performance in spatial learning observed in 18-month-old mice. Binding of insulin to the insulin receptor activates insulin receptor substrate 1 (IRS-1) through phosphorylation. This starts a cascade of reactions whereby IRS-1, in turn, phosphorylates

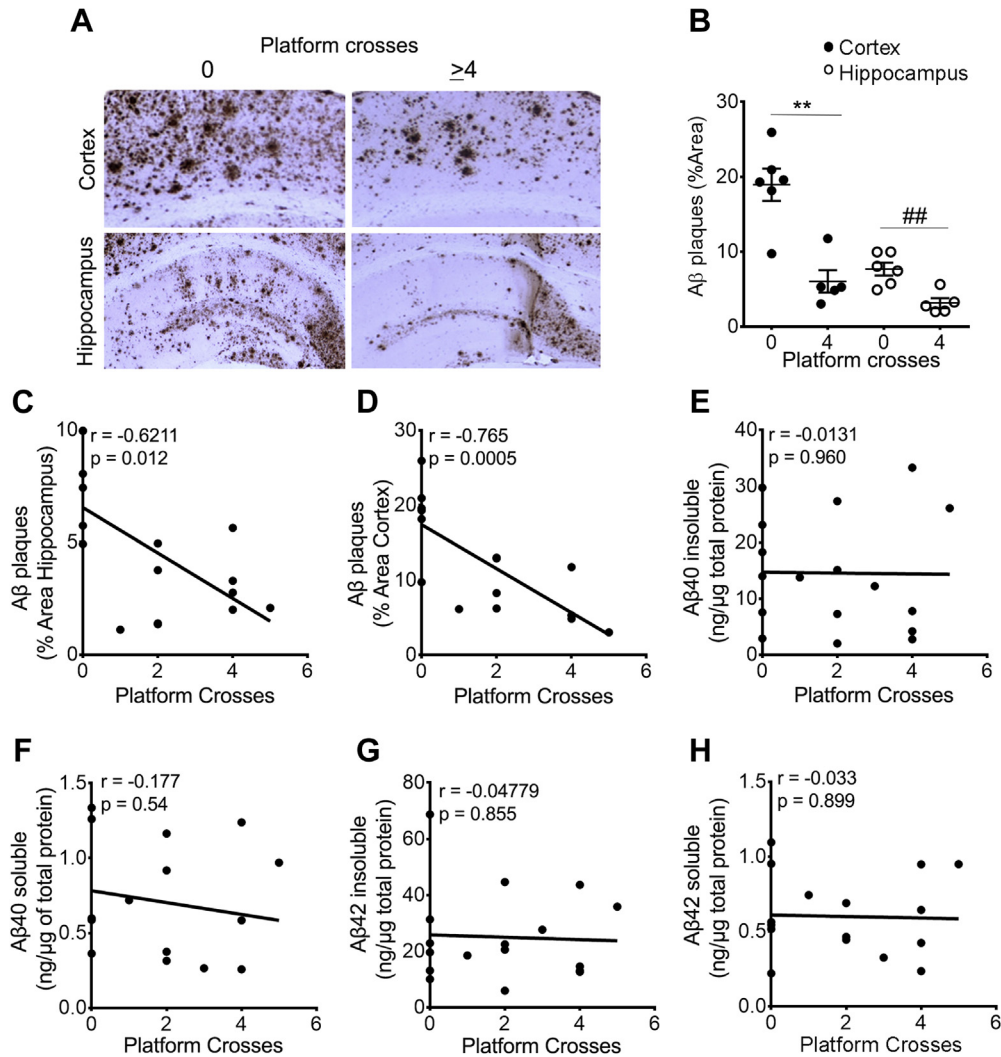


**Fig. 2.** A $\beta$  plaque load strongly correlates with cognitive performance. (A) Representative images of the hippocampus and cortex of 2 groups of APP/PS1 mice: low (zero crosses, n = 6) and high ( $\geq 4$  crosses, n = 5) performers. Sections were stained with a selective A $\beta$ 42 antibody. (B) Plaque load was significantly lower in the high performers compared with the low performers in both the hippocampus and cortex (\*\*  $p < 0.01$  for the hippocampus and ##  $p < 0.01$  for cortex). (C and D) Plaque load in the hippocampus and cortex significantly correlated with platform crosses ( $p < 0.05$  and  $p < 0.001$ , respectively). (E–H) There was no significant correlation between platform crosses and soluble and insoluble A $\beta$ 40 and A $\beta$ 42. The data in panel B were analyzed using unpaired Student's t-test. The data in panels C–H were analyzed using a linear correlation between platform crosses and plaque load or soluble and insoluble A $\beta$ 40/A $\beta$ 42.

phosphoinositide 3 kinase and pyruvate dehydrogenase 1 (PDK1), eventually resulting in phosphorylation of serine/threonine kinase AKT. We measured the levels of total and phosphorylated IRS1 (Ser612), AKT (Thr308 and Ser473), and PDK1 (Ser241) and assessed their correlation with platform crosses in APP/PS1 mice. Overall, we found no significant correlation between activation of insulin signaling and cognitive performance in APP/PS1 mice (Fig. 4A–H). The insulin receptor can also be phosphorylated by 5'AMP-activated protein kinase (Chopra et al., 2012), which is activated by phosphorylation and responds to changes in the ADP/ATP ratio. We measured the levels of total and phosphorylated 5'AMP-activated protein kinase but found no significant correlation with platform crosses in the APP/PS1 mice (Fig. 4A and I–J). These data suggest that the insulin signaling pathway does not correlate with cognitive function in APP/PS1 mice.

#### 3.4. Autophagy is upregulated in mice with better spatial memory

Macroautophagy, herein referred to as autophagy, is an important cellular turnover mechanism that removes aggregated or

damaged proteins. In this process, cytoplasmic proteins and organelles are enveloped in double-membrane vacuoles called autophagosomes. These autophagosomes then combine with lysosomes to degrade their contents (Gkikas et al., 2014). Autophagy is widely reported to be defective in AD, contributing to the deposition of A $\beta$  and tau (Boland et al., 2008; Caccamo et al., 2010; Orr and Oddo, 2013; Yu et al., 2017). To assess autophagy induction, we measured the levels of Beclin-1, Atg5, and Atg7. Beclin-1 contributes to the formation of the autophagosome membrane, and its levels are decreased in AD brains (Kang et al., 2011). Atg5 is necessary to initiate autophagy, whereas Atg7 is critical for the fusion of autophagosomes with the lysosome (Frudd et al., 2018; Liu et al., 2013). In APP/PS1 mice, we found a significant correlation between the number of platform crosses and levels of Beclin-1 ( $r = 0.6457$ ,  $p < 0.01$ ,  $q < 0.05$ ), Atg5 ( $r = 0.765$ ,  $p < 0.01$ ,  $q < 0.05$ ), and Atg7 ( $r = 0.681$ ,  $p < 0.01$ ,  $q < 0.05$ ; Fig. 5A–D, Table 1). In contrast, there was no correlation between platform frequency and Beclin-1, Atg5, or Atg7 in NonTg mice (Supplementary Information, Fig. 1). Overall, these data highlight a correlation between autophagy induction and spatial memory in 18-month-old APP/PS1 mice.

**Table 1**

Adjusted *p*-values for correlation with platform crosses in APP/PS1 mice corrected for multiple testing of hypothesis using Benjamini, Krieger, and Yekutieli method with *Q* = 5%

| Proteins                 | <i>p</i> -value | Adjusted <i>p</i> -value ( <i>q</i> ) |
|--------------------------|-----------------|---------------------------------------|
| p-mTOR                   | 0.0001          | 0.0022                                |
| Aβ plaques (cortex)      | 0.0005          | 0.0055                                |
| Atg5                     | 0.003           | 0.0204                                |
| Atg7                     | 0.0037          | 0.0204                                |
| Beclin 1                 | 0.0051          | 0.0225                                |
| Aβ plaques (hippocampus) | 0.0102          | 0.0375                                |
| p-p70S6K                 | 0.0201          | 0.0633                                |
| p-rps6                   | 0.043           | 0.1185                                |
| mTOR                     | 0.0562          | 0.1372                                |
| Total IRS1               | 0.0622          | 0.1372                                |
| rps6                     | 0.09            | 0.1672                                |
| p-AMPK                   | 0.091           | 0.1672                                |
| Akt                      | 0.125           | 0.212                                 |
| P70S6K                   | 0.143           | 0.2252                                |
| Full-length APP          | 0.162           | 0.2381                                |
| Total PDK1               | 0.324           | 0.4465                                |
| p-PDK1 (241)             | 0.36            | 0.4669                                |
| p-Akt (308)              | 0.467           | 0.5513                                |
| p-IRS1 (612)             | 0.493           | 0.5513                                |
| p-Akt (473)              | 0.5             | 0.5513                                |
| Aβ40 soluble             | 0.54            | 0.567                                 |
| C99                      | 0.7             | 0.6661                                |
| AMPK                     | 0.725           | 0.6661                                |
| C83                      | 0.6             | 0.6014                                |
| Aβ42 insoluble           | 0.855           | 0.7541                                |
| Aβ42 soluble             | 0.899           | 0.7624                                |
| Aβ40 insoluble           | 0.96            | 0.784                                 |

Key: AMPK, 5'AMP-activated protein kinase; APP, amyloid precursor protein; mTOR, mammalian target of rapamycin; PDK1, pyruvate dehydrogenase 1; rps6, ribosomal protein S6.

### 3.5. Reduced mTOR signaling is associated with better spatial memory

The mTOR is a master regulator of autophagy induction, protein translation, and aging. To this end, reducing mTOR activity increases lifespan and health span (Rabanal-Ruiz et al., 2017; Talboom et al., 2015). Converging evidence also indicates that mTOR signaling is involved in aging and AD pathology. Pharmacological

and genetic inhibition of mTOR increases lifespan across various species (Gkikas et al., 2014; Harrison et al., 2009; Jia et al., 2004; Razquin Navas and Thedieck, 2017). Increased mTOR signaling has also been observed in human AD brains (Oddo, 2012). Consistent with these functions, mTOR has also been linked to synaptic plasticity and cognition (Caccamo et al., 2014; Oddo, 2012; Talboom et al., 2015). mTOR activity is routinely assessed by measuring the steady-state levels of ribosomal protein S6 kinase 1 (S6K1) phosphorylated at Thr389, as this epitope is directly phosphorylated by mTOR (Chung et al., 1992). Once phosphorylated, S6K1 regulates protein translation in part by phosphorylating and activating ribosomal protein S6 (rpS6). To assess whether mTOR signaling correlates with cognitive performance in APP/PS1 mice, we measured the total and phosphorylated levels of mTOR, S6K1, and rpS6. We found that the number of platform location crosses negatively correlated with mTOR phosphorylated at Ser2448 ( $r = -0.805$ ,  $p < 0.001$ ,  $q < 0.01$ ; Fig. 6A and C). Although we also found a negative correlation between platform crosses and S6K1 phosphorylated at Thr389 ( $r = -0.557$ ,  $p < 0.05$ ; Fig. 6A–B) and with rpS6 phosphorylated at Ser 240/244 ( $r = -0.495$ ,  $p < 0.05$ ; Fig. 6A–D), these did not hold significance when corrected for multiple testing of hypothesis (Table 1). There was no correlation of platform crosses with total levels of these proteins (Fig. 6A and E–G), indicating that mTOR signaling was upregulated in mice that performed poorly. In contrast, there was also no significant correlation between platform location crosses and mTOR signaling in NonTg mice (Supplementary Information, Fig. 2). Overall, these results identify mTOR signaling as the best predictor of cognitive performance in 18-month-old APP/PS1 mice.

## 4. Discussion

Although much is known regarding the neuropathology of AD, the molecular bases for the cognitive deficits associated with this disorder remain poorly understood. Numerous studies point to either the Aβ (Foley et al., 2015; Huber et al., 2018; Malek-Ahmadi et al., 2016) or tau pathology (Huber et al., 2018; Kosik et al., 1986) along with synaptic loss and neurodegeneration as the culprit for cognitive deficits seen in AD. In this study, we used 18-month-old APP/PS1 mice to identify the underlying pathways for

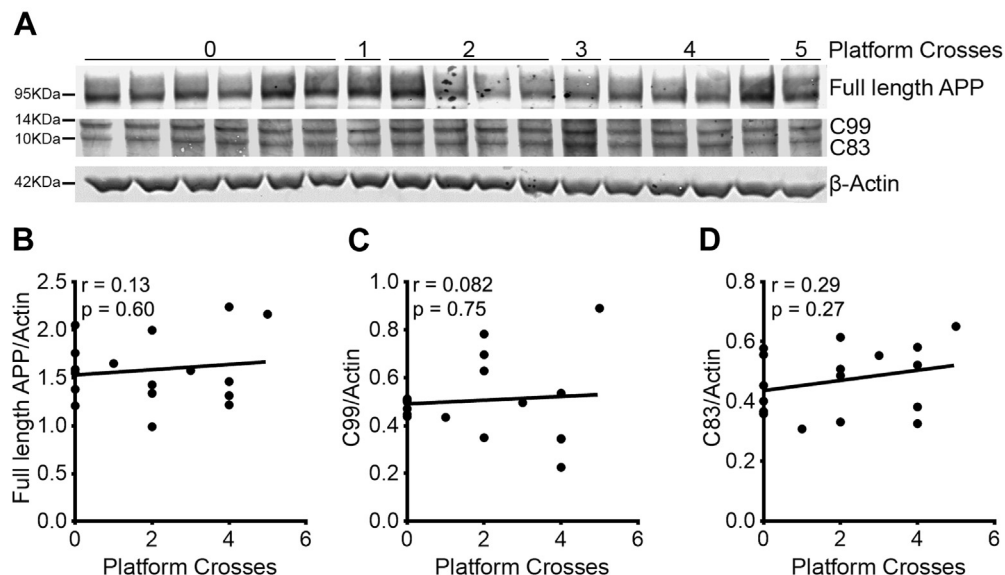


**Fig. 3.** APP processing does not correlate with spatial memory. (A) Western blot images of full-length APP and its major C-terminal fragments, C99, and C83 in APP/PS1 mice ranging from zero to 5 platform crosses (APP/PS1 mice, *n* = 17). (B–D) The number of platform crosses did not correlate with full-length APP, C99, and C83. The data were analyzed using linear correlation. Abbreviation: APP, amyloid precursor protein.

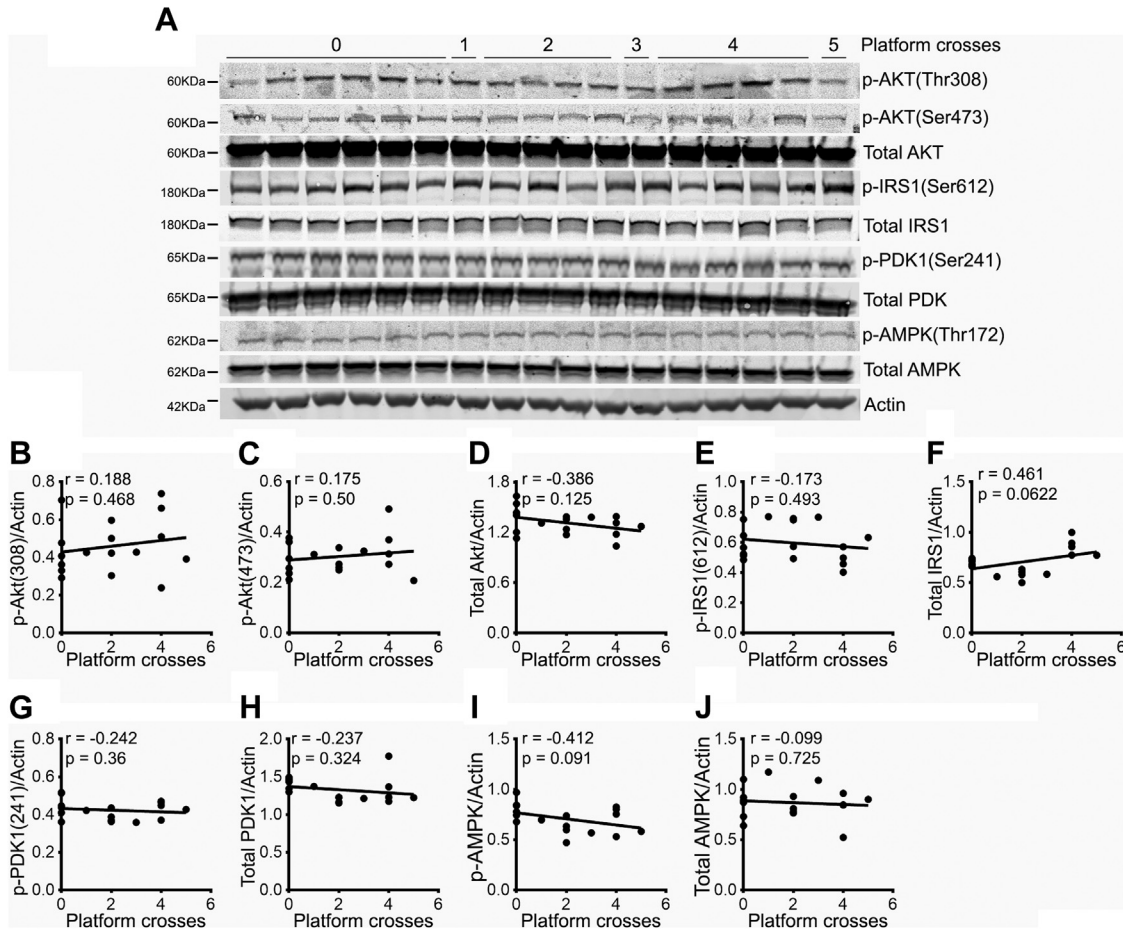


**Fig. 4.** Insulin signaling does not correlate with special memory in APP/PS1 mice. (A) Western blot of total and phosphorylated AKT, IRS1, PDK1, and AMPK $\alpha$  in APP/PS1 mice ranging from zero to 5 platform crosses (APP/PS1 mice, n = 17). (B–J) Spatial memory did not correlate with markers of insulin signaling. The data were analyzed using linear correlation analysis.

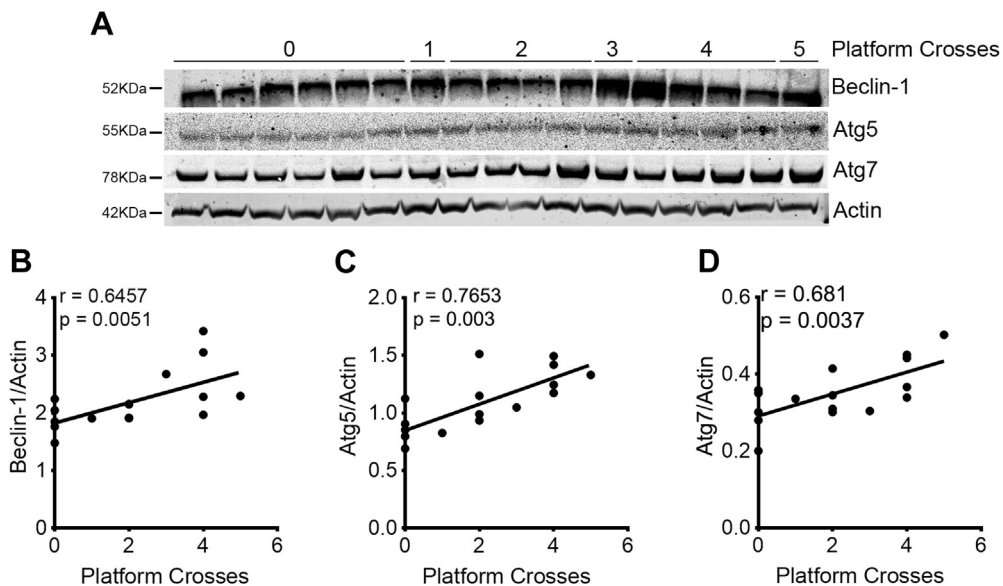


**Fig. 5.** Autophagy induction is upregulated in APP/PS1 mice with better spatial memory. (A) Representative Western blot images of Beclin-1, Atg5, and Atg7 in APP/PS1 mice ranging from zero to 5 platform crosses (APP/PS1 mice, n = 17). (B–D) The steady-state levels of all 3 proteins significantly correlated with spatial memory.  $p < 0.01$  for all autophagy markers. The data were analyzed using a linear correlation between platform crosses and autophagy markers.

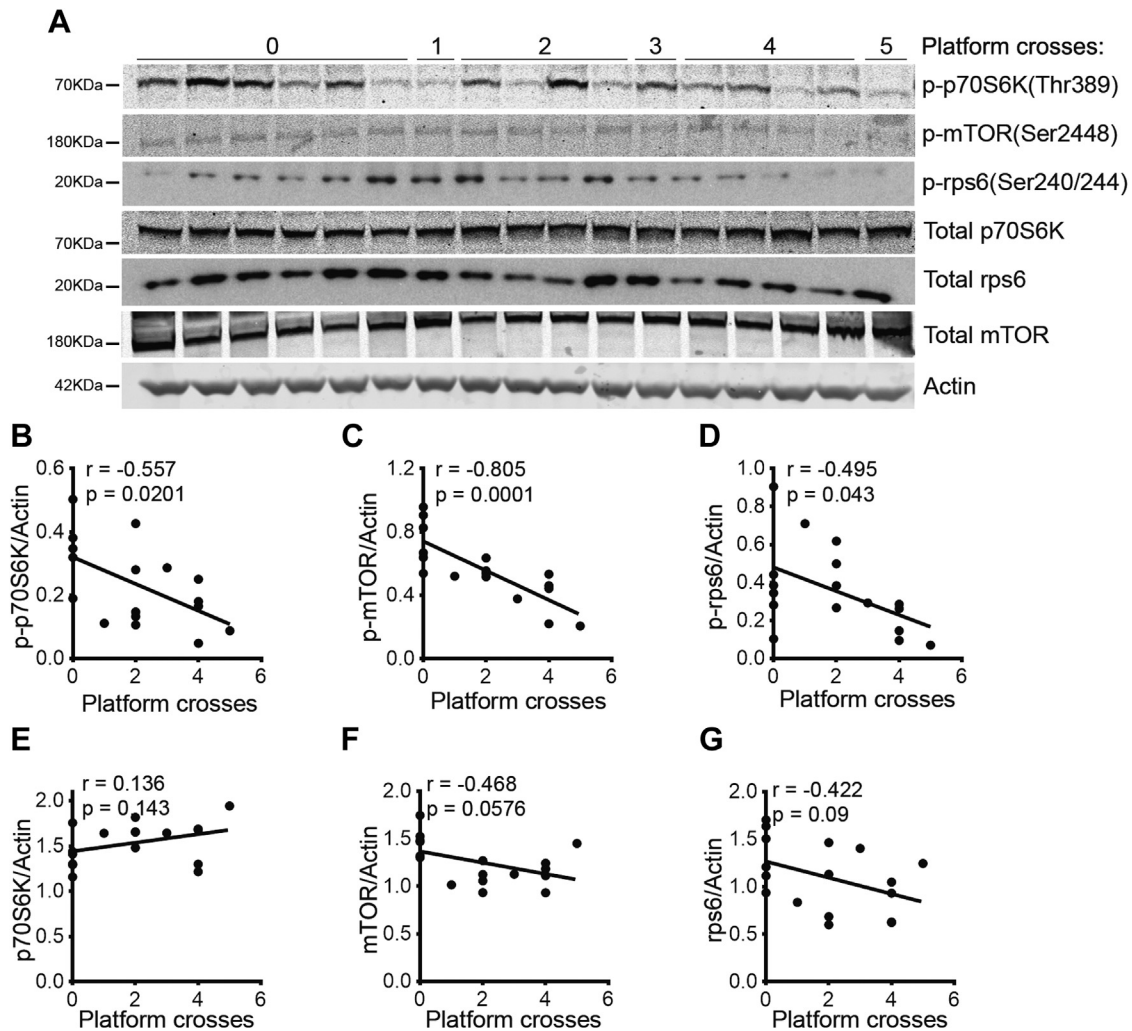


**Fig. 6.** mTOR signaling inversely correlates with spatial memory in APP/PS1 mice. (A) Representative Western blot images of total and phosphorylated S6K1, mTOR, rpS6 in APP/PS1 mice ranging from zero to 5 platform crosses (APP/PS1 mice,  $n = 17$ ). (B–D) Spatial memory significantly and inversely correlated with pS6K1 ( $p < 0.05$ ), p-mTOR ( $p < 0.001$ ), and p-rpS6 ( $p < 0.05$ ). (E–G) Spatial memory did not correlate with the total levels of S6K1, mTOR, and rpS6. The data were analyzed using a linear correlation between platform crosses and markers of mTOR signaling. Abbreviation: mTOR, mammalian target of rapamycin.

cognitive dysfunction in AD. Commonly, many studies have used comparisons between APP/PS1 mice and NonTg to understand the molecular differences that give rise to cognitive deficits. Although these studies have led to the identification of critical mechanisms of disease pathogenesis, using intragroup variability to identify pathways associated with cognitive deficits would remove several confounding variables from the analyses.

We used the MWM to test spatial learning and memory in the APP/PS1 mice. Consistent with previous reports, we found a significant reduction in spatial memory in APP/PS1 mice as compared to the NonTg mice (Caccamo et al., 2017; Webster et al., 2014). However, within the APP/PS1 group, we observed a wide variation in the number of platform location crosses (an indication of spatial memory), with some of the APP/PS1 mice showing profound deficits while others were performing as well as NonTg mice. Previous studies have found that soluble A $\beta$ , as well as A $\beta$  plaques, may indirectly affect cognition by causing synaptic dysfunction and neuronal loss (Huber et al., 2018; Malek-Ahmadi et al., 2016; Selkoe, 2008). We found that cognitive deficits in the APP/PS1 mice correlate strongly with A $\beta$  plaque load across the hippocampus and cortex. However, we found no correlation between cognitive function and soluble/insoluble A $\beta$ 40 and A $\beta$ 42. Although many

studies find a strong correlation between soluble A $\beta$  and early AD pathogenesis, the levels of soluble A $\beta$  decrease drastically in aged AD brains as insoluble and fibrillar A $\beta$ 42 increases (Koss et al., 2016; Wang et al., 1999). It is thus possible that the plaque burden in aged 18-month-old APP/PS1 mice is so severe that the differences in soluble A $\beta$  levels are not apparent, and therefore, we see no correlation with cognition. In addition, targeting soluble A $\beta$  levels therapeutically in humans did not prevent cognitive dysfunction (Honig et al., 2018), suggesting that the link between soluble A $\beta$  and cognition is not as straightforward as initially thought.

mTOR signaling is linked to synaptic plasticity, memory formation, and cognition (Bekinschtein et al., 2007; Bockaert and Marin, 2015; Gafford et al., 2011; Oddo, 2012; Pereyra et al., 2018; Talboom et al., 2015). To this end, mTOR signaling is needed for memory consolidation (Casadio et al., 1999; Tischmeyer et al., 2003). mTOR signaling has also been implicated in cognitive aging by increasing protein translation and decreasing autophagy causing synaptic degeneration and cognitive defects. However, hyperactive mTOR signaling is detrimental for learning and memory as indicated by studies in a mouse model of tuberous sclerosis (Ehninger et al., 2008). Consistent with these observations, long-term rapamycin treatment improves cognition and spatial memory (Caccamo et al.,

2010; Halloran et al., 2012; Majumder et al., 2012). A link between mTOR hyperactivity and cognitive impairment has also been observed in Down syndrome and AD (Caccamo et al., 2014, 2015; Iyer et al., 2014; Oddo, 2012). Removing a single copy of mTOR ameliorates the AD pathology and improve cognition in mice, underlining the link between mTOR hyperactivity and cognitive deficits (Caccamo et al., 2014). Interestingly, we found that mTOR, and consequently autophagy is differentially activated in APP/PS1 mice with better spatial memory. The correlation between cognitive function and mTOR activity is specific only to APP/PS1 mice as there was no correlation between mTOR activity, autophagy, and cognition in the NonTg mice. This finding has important implications for mTOR and autophagy in cognitive aging. Our results suggest that mTOR activity and autophagy has a stronger link to cognitive deficits in the context of neurodegenerative diseases than natural cognitive aging. It can be hypothesized that since APP/PS1 mice have increased A $\beta$  load, a modest increase in autophagy may lead to better cognitive outcomes than in NonTg mice. Overall, our study shows that within the cohort of 18-month-old APP/PS1 mice, there may be a differential regulation of the mTOR pathway and autophagy, which leads to different performance in spatial memory. We hypothesize that reduced mTOR activity results in increased autophagy which further reduces the A $\beta$  plaques. Each of these factors can, in turn, affect overall neuronal health resulting in improved cognition. Our results suggest that markers of autophagy and mTOR activation may be used as a measure of cognitive function in AD animal models.

## Disclosure

The authors do not have any conflict of interests or financial interest in this work. None of the author's institutions have contracts relating to this research through which it or any other organization may stand to gain financially now or in the future.

## Acknowledgements

This work was supported by grants from the Arizona Alzheimer's Consortium to SO and the National Institutes of Health to SO (RF1 AG037637; R01 AG057596).

## Appendix A. Supplementary data

Supplementary data to this article can be found online at <https://doi.org/10.1016/j.neurobiolaging.2019.08.018>.

## References

- Alzheimer's Association, 2016. 2016 Alzheimer's disease facts and figures. *Alzheimer's Dement.* 12, 459–509.
- An, W.L., Cowburn, R.F., Li, L., Braak, H., Alafuzoff, I., Iqbal, K., Iqbal, I.G., Winblad, B., Pei, J.J., 2003. Up-regulation of phosphorylated/activated p70 S6 kinase and its relationship to neurofibrillary pathology in Alzheimer's disease. *Am. J. Pathol.* 163, 591–607.
- Bekinschtein, P., Katche, C., Slipczuk, L.N., Igaz, L.M., Cammarota, M., Izquierdo, I., Medina, J.H., 2007. mTOR signaling in the hippocampus is necessary for memory formation. *Neurobiol. Learn. Mem.* 87, 303–307.
- Belfiore, R., Rodin, A., Ferreira, E., Velazquez, R., Branca, C., Caccamo, A., Oddo, S., 2019. Temporal and regional progression of Alzheimer's disease-like pathology in 3xTg-AD mice. *Aging Cell* 18, e12873.
- Bjedov, I., Toivonen, J.M., Kerr, F., Slack, C., Jacobson, J., Foley, A., Partridge, L., 2010. Mechanisms of life span extension by rapamycin in the fruit fly *Drosophila melanogaster*. *Cell Metab.* 11, 35–46.
- Bockaert, J., Marin, P., 2015. mTOR in brain physiology and pathologies. *Physiol. Rev.* 95, 1157–1187.
- Boland, B., Kumar, A., Lee, S., Platt, F.M., Wegiel, J., Yu, W.H., Nixon, R.A., 2008. Autophagy induction and autophagosome clearance in neurons: relationship to autophagic pathology in Alzheimer's disease. *J. Neurosci.* 28, 6926–6937.
- Branca, C., Wisely, E.V., Hartman, L.K., Caccamo, A., Oddo, S., 2014. Administration of a selective beta2 adrenergic receptor antagonist exacerbates neuropathology and cognitive deficits in a mouse model of Alzheimer's disease. *Neurobiol. Aging* 35, 2726–2735.
- Caccamo, A., Majumder, S., Richardson, A., Strong, R., Oddo, S., 2010. Molecular interplay between mammalian target of rapamycin (mTOR), amyloid-beta, and Tau: effects on cognitive impairments. *J. Biol. Chem.* 285, 13107–13120.
- Caccamo, A., Magri, A., Medina, D.X., Wisely, E.V., Lopez-Aranda, M.F., Silva, A.J., Oddo, S., 2013. mTOR regulates tau phosphorylation and degradation: implications for Alzheimer's disease and other tauopathies. *Aging Cell* 12, 370–380.
- Caccamo, A., De Pinto, V., Messina, A., Branca, C., Oddo, S., 2014. Genetic reduction of mammalian target of rapamycin ameliorates Alzheimer's disease-like cognitive and pathological deficits by restoring hippocampal gene expression signature. *J. Neurosci.* 34, 7988–7998.
- Caccamo, A., Branca, C., Talboom, J.S., Shaw, D.M., Turner, D., Ma, L., Messina, A., Huang, Z., Wu, J., Oddo, S., 2015. Reducing ribosomal protein S6 kinase 1 expression improves spatial memory and synaptic plasticity in a mouse model of Alzheimer's disease. *J. Neurosci.* 35, 14042–14056.
- Caccamo, A., Ferreira, E., Branca, C., Oddo, S., 2017. p62 improves AD-like pathology by increasing autophagy. *Mol. Psychiatry* 22, 865–873.
- Caccamo, A., Belfiore, R., Oddo, S., 2018. Genetically reducing mTOR signaling rescues central insulin dysregulation in a mouse model of Alzheimer's disease. *Neurobiol. Aging* 68, 59–67.
- Casadio, A., Martin, K.C., Giustetto, M., Zhu, H., Chen, M., Bartsch, D., Bailey, C.H., Kandel, E.R., 1999. A transient, neuron-wide form of CREB-mediated long-term facilitation can be stabilized at specific synapses by local protein synthesis. *Cell* 99, 221–237.
- Chopra, I., Li, H.F., Wang, H., Webster, K.A., 2012. Phosphorylation of the insulin receptor by AMP-activated protein kinase (AMPK) promotes ligand-independent activation of the insulin signalling pathway in rodent muscle. *Diabetologia* 55, 783–794.
- Chung, J., Kuo, C.J., Crabtree, G.R., Blenis, J., 1992. Rapamycin-FKBP specifically blocks growth-dependent activation of and signaling by the 70 kd S6 protein kinases. *Cell* 69, 1227–1236.
- Ehninger, D., Han, S., Shilyansky, C., Zhou, Y., Li, W., Kwiatkowski, D.J., Ramesh, V., Silva, A.J., 2008. Reversal of learning deficits in a *Tsc2*<sup>-/-</sup> mouse model of tuberous sclerosis. *Nat. Med.* 14, 843–848.
- Folch, J., Etcheto, M., Busquets, O., Sánchez-López, E., Castro-Torres, R.D., Verdager, E., Manzone, P.R., Poor, S.R., García, M.L., Olloquequi, J., Beas-Zarate, C., Auladell, C., Camins, A., 2018. The implication of the brain insulin receptor in late onset Alzheimer's disease dementia. *Pharmaceuticals (Basel)* 11.
- Foley, A.M., Ammar, Z.M., Lee, R.H., Mitchell, C.S., 2015. Systematic review of the relationship between amyloid- $\beta$  levels and measures of transgenic mouse cognitive deficit in Alzheimer's disease. *J. Alzheimers Dis.* 44, 787–795.
- Frudd, K., Burgoyne, T., Burgoyne, J.R., 2018. Oxidation of Atg3 and Atg7 mediates inhibition of autophagy. *Nat. Commun.* 9, 95.
- Gafford, G.M., Parsons, R.G., Helmstetter, F.J., 2011. Consolidation and reconsolidation of contextual fear memory requires mammalian target of rapamycin-dependent translation in the dorsal hippocampus. *Neuroscience* 182, 98–104.
- Gkikas, I., Petratou, D., Tavernarakis, N., 2014. Longevity pathways and memory aging. *Front. Genet.* 5, 155.
- Halloran, J., Hussong, S.A., Burbank, R., Podlutzkaya, N., Fischer, K.E., Sloane, L.B., Austad, S.N., Strong, R., Richardson, A., Hart, M.J., Galvan, V., 2012. Chronic inhibition of mammalian target of rapamycin by rapamycin modulates cognitive and non-cognitive components of behavior throughout lifespan in mice. *Neuroscience* 223, 102–113.
- Harrison, D.E., Strong, R., Sharp, Z.D., Nelson, J.F., Astle, C.M., Flurkey, K., Nadon, N.L., Wilkinson, J.E., Frenkel, K., Carter, C.S., Pahor, M., Javors, M.A., Fernandez, E., Miller, R.A., 2009. Rapamycin fed late in life extends lifespan in genetically heterogeneous mice. *Nature* 460, 392–395.
- Hebert, L.E., Weuve, J., Scherr, P.A., Evans, D.A., 2013. Alzheimer disease in the United States (2010–2050) estimated using the 2010 census. *Neurology* 80, 1778–1783.
- Honig, L.S., Vellas, B., Woodward, M., Boada, M., Bullock, R., Borrie, M., Hager, K., Andreasen, N., Scarpini, E., Liu-Seifert, H., Case, M., Dean, R.A., Hake, A., Sundell, K., Poole Hoffmann, V., Carlson, C., Khanna, R., Mintun, M., DeMattos, R., Selzler, K.J., Siemers, E., 2018. Trial of Solanezumab for mild dementia due to Alzheimer's disease. *N. Engl. J. Med.* 378, 321–330.
- Huber, C.M., Yee, C., May, T., Dhanala, A., Mitchell, C.S., 2018. Cognitive decline in preclinical Alzheimer's disease: amyloid-beta versus Tauopathy. *J. Alzheimers Dis.* 61, 265–281.
- Iyer, A.M., van Scheppingen, J., Milenkovic, I., Anink, J.J., Adle-Biassette, H., Kovacs, G.G., Aronica, E., 2014. mTOR Hyperactivation in down syndrome hippocampus appears early during development. *J. Neuropathol. Exp. Neurol.* 73, 671–683.
- Jankowsky, J.L., Fadale, D.J., Anderson, J., Xu, G.M., Gonzales, V., Jenkins, N.A., Copeland, N.G., Lee, M.K., Younkin, L.H., Wagner, S.L., Younkin, S.G., Borchelt, D.R., 2004. Mutant presenilins specifically elevate the levels of the 42 residue beta-amyloid peptide in vivo: evidence for augmentation of a 42-specific gamma secretase. *Hum. Mol. Genet.* 13, 159–170.
- Jia, K., Chen, D., Riddle, D.L., 2004. The TOR pathway interacts with the insulin signaling pathway to regulate *C. elegans* larval development, metabolism and life span. *Development* 131, 3897–3906.
- Kang, R., Zeh, H.J., Lotze, M.T., Tang, D., 2011. The Beclin 1 network regulates autophagy and apoptosis. *Cell Death Differ* 18, 571–580.
- Kenyon, C., Chang, J., Gensch, E., Rudner, A., Tabtiang, R., 1993. A *C. elegans* mutant that lives twice as long as wild type. *Nature* 366, 461–464.

- Kosik, K.S., Joachim, C.L., Selkoe, D.J., 1986. Microtubule-associated protein tau ( $\tau$ ) is a major antigenic component of paired helical filaments in Alzheimer disease. *Proc. Natl. Acad. Sci. U. S. A.* 83, 4044–4048.
- Koss, D.J., Jones, G., Cranston, A., Gardner, H., Kanaan, N.M., Platt, B., 2016. Soluble pre-fibrillar tau and  $\beta$ -amyloid species emerge in early human Alzheimer's disease and track disease progression and cognitive decline. *Acta Neuropathol.* 132, 875–895.
- Lafay-Chebassier, C., Paccalin, M., Page, G., Barc-Pain, S., Perault-Pochat, M.C., Gil, R., Pradier, L., Hugon, J., 2005. mTOR/p70S6k signalling alteration by Abeta exposure as well as in APP-PS1 transgenic models and in patients with Alzheimer's disease. *J. Neurochem.* 94, 215–225.
- Li, X., Alafuzoff, I., Soininen, H., Winblad, B., Pei, J.J., 2005. Levels of mTOR and its downstream targets 4E-BP1, eEF2, and eEF2 kinase in relationships with tau in Alzheimer's disease brain. *FEBS J.* 272, 4211–4220.
- Liu, H., He, Z., von Rütte, T., Yousefi, S., Hunger, R.E., Simon, H.U., 2013. Down-regulation of autophagy-related protein 5 (ATG5) contributes to the pathogenesis of early-stage cutaneous melanoma. *Sci. Transl. Med.* 5, 202ra123.
- Majumder, S., Caccamo, A., Medina, D.X., Benavides, A.D., Javors, M.A., Kraig, E., Strong, R., Richardson, A., Oddo, S., 2012. Lifelong rapamycin administration ameliorates age-dependent cognitive deficits by reducing IL-1 $\beta$  and enhancing NMDA signaling. *Aging Cell* 11, 326–335.
- Malek-Ahmadi, M., Perez, S.E., Chen, K., Mufson, E.J., 2016. Neuritic and diffuse plaque associations with memory in non-cognitively impaired elderly. *J. Alzheimers Dis.* 53, 1641–1652.
- Masters, C.L., Bateman, R., Blennow, K., Rowe, C.C., Sperling, R.A., Cummings, J.L., 2015. Alzheimer's disease. *Nat. Rev. Dis. Primers* 1, 15056.
- Nelson, P.T., Braak, H., Markesbery, W.R., 2009. Neuropathology and cognitive impairment in Alzheimer disease: a complex but coherent relationship. *J. Neuropathol. Exp. Neurol.* 68, 1–14.
- Norambuena, A., Wallrabe, H., McMahon, L., Silva, A., Swanson, E., Khan, S.S., Baerthlein, D., Kodis, E., Oddo, S., Mandell, J.W., Bloom, G.S., 2017. mTOR and neuronal cell cycle reentry: how impaired brain insulin signaling promotes Alzheimer's disease. *Alzheimers Dement.* 13, 152–167.
- Oddo, S., 2012. The role of mTOR signaling in Alzheimer disease. *Front Biosci. (Schol Ed)* 4, 941–952.
- Orr, M.E., Oddo, S., 2013. Autophagic/lysosomal dysfunction in Alzheimer's disease. *Alzheimers Res. Ther.* 5, 53.
- Orr, M.E., Salinas, A., Buffenstein, R., Oddo, S., 2014. Mammalian target of rapamycin hyperactivity mediates the detrimental effects of a high sucrose diet on Alzheimer's disease pathology. *Neurobiol. Aging* 35, 1233–1242.
- Pereyra, M., Katche, C., de Landeta, A.B., Medina, J.H., 2018. mTORC1 controls long-term memory retrieval. *Sci. Rep.* 8, 8759.
- Rabanal-Ruiz, Y., Otten, E.G., Korolchuk, V.I., 2017. mTORC1 as the main gateway to autophagy. *Essays Biochem.* 61, 565–584.
- Radde, R., Bolmont, T., Kaeser, S.A., Coomaraswamy, J., Lindau, D., Stoltze, L., Calhoun, M.E., Jäggi, F., Wolburg, H., Gengler, S., Haass, C., Ghetti, B., Czech, C., Hölscher, C., Mathews, P.M., Jucker, M., 2006. Abeta42-driven cerebral amyloidosis in transgenic mice reveals early and robust pathology. *EMBO Rep.* 7, 940–946.
- Razquin Navas, P., Thedieck, K., 2017. Differential control of ageing and lifespan by isoforms and splice variants across the mTOR network. *Essays Biochem.* 61, 349–368.
- Richardson, A., Galvan, V., Lin, A.L., Oddo, S., 2015. How longevity research can lead to therapies for Alzheimer's disease: the rapamycin story. *Exp. Gerontol.* 68, 51–58.
- Rodriguez-Rivera, J., Denner, L., Dineley, K.T., 2011. Rosiglitazone reversal of Tg2576 cognitive deficits is independent of peripheral gluco-regulatory status. *Behav. Brain Res.* 216, 255–261.
- Selkoe, D.J., 2008. Soluble oligomers of the amyloid beta-protein impair synaptic plasticity and behavior. *Behav. Brain Res.* 192, 106–113.
- Serneels, L., Van Biervliet, J., Craessaerts, K., Dejaegere, T., Horr , K., Van Houtvin, T., Esselmann, H., Paul, S., Sch fer, M.K., Berezovska, O., Hyman, B.T., Sprangers, B., Sciot, R., Moons, L., Jucker, M., Yang, Z., May, P.C., Karran, E., Wiltfang, J., D'Hooge, R., De Strooper, B., 2009. gamma-secretase heterogeneity in the Aph1 subunit: relevance for Alzheimer's disease. *Science* 324, 639–642.
- Talboom, J.S., Velazquez, R., Oddo, S., 2015. The mammalian target of rapamycin at the crossroad between cognitive aging and Alzheimer's disease. *NPJ Aging Mech. Dis.* 1, 15008.
- Tischmeyer, W., Schicknick, H., Kraus, M., Seidenbecher, C.I., Staak, S., Scheich, H., Gundelfinger, E.D., 2003. Rapamycin-sensitive signalling in long-term consolidation of auditory cortex-dependent memory. *Eur. J. Neurosci.* 18, 942–950.
- Velazquez, R., Tran, A., Ishimwe, E., Denner, L., Dave, N., Oddo, S., Dineley, K.T., 2017. Central insulin dysregulation and energy dyshomeostasis in two mouse models of Alzheimer's disease. *Neurobiol. Aging* 58, 1–13.
- Wang, J., Dickson, D.W., Trojanowski, J.Q., Lee, V.M., 1999. The levels of soluble versus insoluble brain Abeta distinguish Alzheimer's disease from normal and pathologic aging. *Exp. Neurol.* 158, 328–337.
- Webster, S.J., Bachstetter, A.D., Nelson, P.T., Schmitt, F.A., Van Eldik, L.J., 2014. Using mice to model Alzheimer's dementia: an overview of the clinical disease and the preclinical behavioral changes in 10 mouse models. *Front Genet.* 5, 88.
- Wullschleger, S., Loewith, R., Hall, M.N., 2006. TOR signaling in growth and metabolism. *Cell* 124, 471–484.
- Yu, Y., Feng, L., Li, J., Lan, X., A, L., Lv, X., Zhang, M., Chen, L., 2017. The alteration of autophagy and apoptosis in the hippocampus of rats with natural aging-dependent cognitive deficits. *Behav. Brain Res.* 334, 155–162.